Comparative ^{13}C-NMR and Matrix-Assisted Laser Desorption/Ionization Time-of-Flight Analyses of Species Variation and Structure Maintenance During Melamine–Urea–Formaldehyde Resin Preparation

A. Despres,[1] A. Pizzi,[1] H. Pasch,[2] A. Kandelbauer[3]

[1]*ENSTIB-LERMAB, University of Nancy 1, Epinal, France*
[2]*Analytical Department, Deutsche Kunststoffe Institut, Darmstadt, Germany*
[3]*Wood-K Plus, Kompetenzzentrum Holz GmbH, A-9300 Saint Vait an der Glan, Austria*

Received 29 November 2006; accepted 14 March 2007
DOI 10.1002/app.26573
Published online 8 July 2007 in Wiley InterScience (www.interscience.wiley.com).

ABSTRACT: The preparation of an industrially used sequential formulation of a melamine–urea–formaldehyde resin was followed by matrix-assisted laser desorption/ionization time-of-flight mass spectrometry and ^{13}C-NMR analysis. The analysis allowed us to identify and follow the appearance, increase, decrease, and disappearance of a multitude of chemical species during the preparation of both the initial urea–formaldehyde (UF) phase of the reaction and the subsequent reaction of melamine with the UF resin that formed. The analysis indicated that (1) the increase and decrease in the species that formed proceeded through a cycle of the formation and degradation of species occurring continuously through what appeared to be a series of complex equilibria, (2) even at the end of the reaction a predominant proportion of methylene ether bridges was still present, (3) some small proportion of methylene bridges already had formed in the UF reaction phase of the resin even under rather alkaline conditions, and (4) the addition of melamine to the UF prepolymer induced some noticeable rearrangement of methylene ether bridges to methylene bridges. © 2007 Wiley Periodicals, Inc. J Appl Polym Sci 106: 1106–1128, 2007

Key words: adhesives; mass spectrometry; NMR; resins; structure

INTRODUCTION

Melamine–urea–formaldehyde (MUF) thermosetting resins are extensively used as exterior-grade adhesives in the wood industry, particularly in the wood-panel industry.[1] The wood-panel industry relies heavily on the use of these synthetic resins as adhesives, bonded products constituting the majority of the wood products on the market today. Over many years, excellent formulations have been developed for these resins for wood applications. Although some trial-and-error industrial research has been and is still carried out in the field of resin formulations, resin knowledge has progressed to such an extent that scientific principles are used today to develop resins of ever-improving performance.

Notwithstanding the considerable tonnage of MUF resins produced yearly, their economic importance, and the trade literature on the subject, the scientific literature on MUF resins is still rather limited.[2–5] This has improved in the last few years. However, much remains to be defined in the field of MUF resins. Only recently has a study appeared that follows the development of the different mass fractions and, by inference, the average molecular species development as a function of the type of formulation used.[6] No study, however, has been performed on what different chemical species are formed during the preparation of MUF resins and how they evolve throughout the complete preparation procedure of the resins. Although a great variety of MUF formulations exist and are used industrially, the greater majority of them are produced according to so-called sequential formulations, in which the sequence of addition of chemicals follows well-defined species reactivity principles.[2–5] The greater majority of MUF resins falls into this category, as these resins produce real cocondensates of melamine and urea and their performance is good.[3–5]

This article deals then with the different chemical species that form and their distribution throughout the preparation of an industrially used MUF resin sequential formulation by analyzing the relevant fractions with ^{13}C-NMR and matrix-assisted laser desorption/ionization time-of-flight (MALDI-TOF) mass spectrometry.

EXPERIMENTAL

Resin preparation

MUF resins with an (M + U)/F molar ratio of 1 : 1.2 and an M/U weight ratio of 47 : 53 (where M is mela-

Correspondence to: A. Pizzi (pizzi@enstib.uhp-nancy.fr).

Journal of Applied Polymer Science, Vol. 106, 1106–1128 (2007)

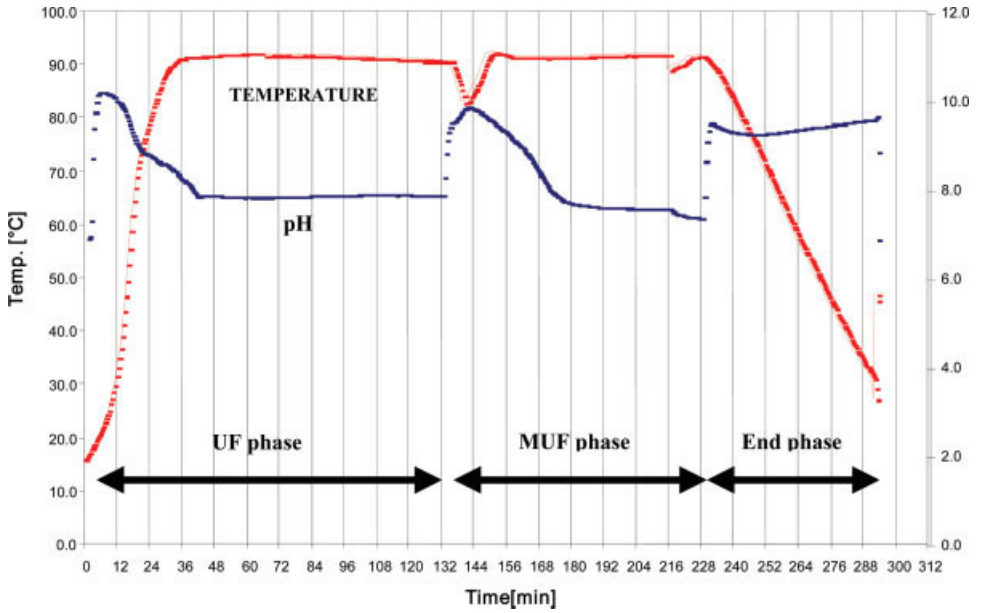

Figure 1 Schematic preparation diagram of an MUF resin showing the temperature and pH variations as functions of the reaction time. [Color figure can be viewed in the online issue, which is available at www.interscience.wiley.com.]

mine, U is urea, and F is formaldehyde) were prepared according to a modification of a known sequential manufacturing procedures[7] as follows: To 71.11 parts of formurea (a precondensate that was 23% urea, 54% formaldehyde, and 23% water) were added 8.18 parts of urea and 15 parts of water. The pH was set at 10–10.4, and the temperature was brought to 92–93°C under mechanical stirring. The pH was then lowered to 7.8, and the reaction was continued at the same temperature. To bring the pH to 9.5 or higher, a 22% NaOH solution was added, and this was followed by 40.0 parts of melamine premixed with 21.0 parts of water. Two parts of dimethylformamide were then added to the reaction mixture, and a temperature of 93°C was maintained. The water tolerance (%) of the resin was checked every 10 min while the pH was allowed to fall by itself back down to 7.4–7.6. When the water tolerance (the percentage of water that could be added to the liquid resin) reached a value of 180–200% (the pH was ca. 7.2), 21.4 parts of urea together with 5 parts water were added, and the pH was again brought up to 9.5. The reaction was continued until the water tolerance was lower than 150% (the pH reached 7.7 at this stage).

The pH was then corrected to 10.0–10.2 by the addition of a solution of NaOH, and the resin was cooled and stored.

The reaction times of each phase according to the outlined procedure are shown in Figure 1.

The times at which the samples were taken, reported on the scale in Figure 1, were as follows:

Sample 1: 5 min after the start of the reaction.
Sample 2: 36 min and when the temperature reached 92°C.
Sample 5: 130 min and 10 min before the melamine addition.
Sample 7: 149 min and 10 min after the melamine addition.
Sample 10: 195 min, 56 min after the melamine addition, and 21 min before the last urea addition.
Sample 11: 210 min, 71 min after the melamine addition, and 6 min before the last urea addition.
Sample 12: 216 min and immediately after the last urea addition.
Sample 13: 226 min and as the temperature rebounded to 92°C.
Sample 14: 287 min and the end of the reaction.

MALDI-TOF mass spectrometry

The MALDI-TOF mass spectra were recorded on a Kratos Kompact MALDI 4 instrument (Shimadzu Corporation, Kyoto, Japan). The irradiation source was a pulsed nitrogen laser with a wavelength of 337 nm. The length of one laser pulse was 3 ns. The measurements were carried out under the following conditions: a positive polarity, a linear flight path, a high mass (20-kV acceleration voltage), and 100–150 pulses per spectrum. The delayed extraction technique was used with delay times of 200–800 ns.

MALDI-TOF sample preparation

The samples were dissolved in water (4 mg/mL). The sample solutions were mixed with an acetone solution (10 mg/mL acetone) of the matrix. As the

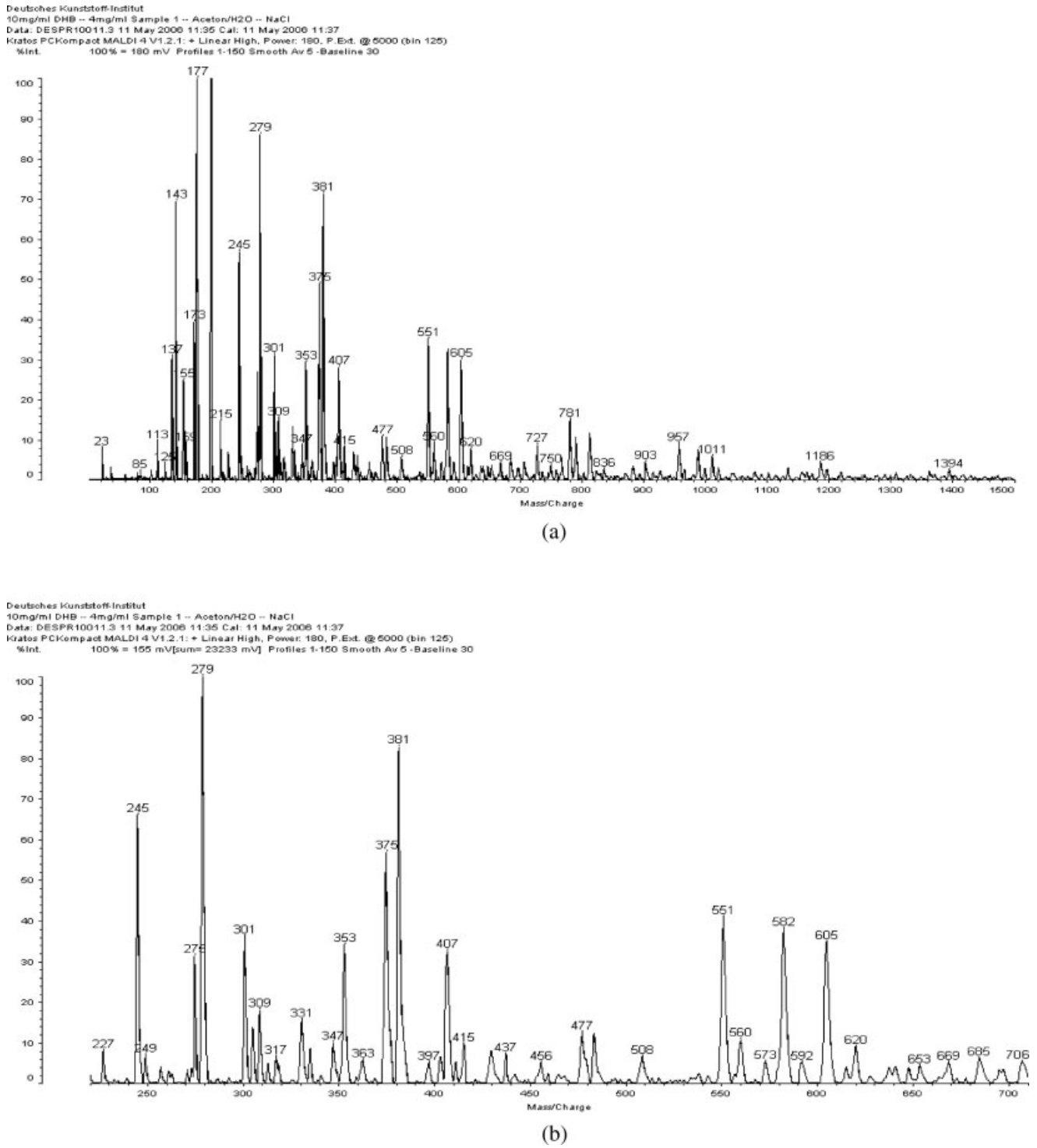

Figure 2 MALDI-TOF spectra of MUF sample 1: (a) the 1–1500-Da region and (b) a detail of the 220–710-Da region.

matrix, dithranol was used. NaCl was not added to the matrix. The solutions of the sample and the matrix were mixed in equal amounts, and 0.5–1 μL of the resulting solution was placed on the MALDI target. After the evaporation of the solvent, the MALDI target was introduced into the spectrometer. The mass peaks corresponded to M + Na (from natural abundance) and M + H attached cations.

^{13}C-NMR

The liquid ^{13}C-NMR spectrum of the PF resin used was obtained on a Brüker MSL 300 FT-NMR spectrometer (Brüker, Wissembourg, France). The chemical shifts were calculated with respect to $(CH_3)_3Si(CH_2)_3SO_3Na$ dissolved in D_2O for NMR shift control.[3,4] The spectra were taken at 62.90 MHz

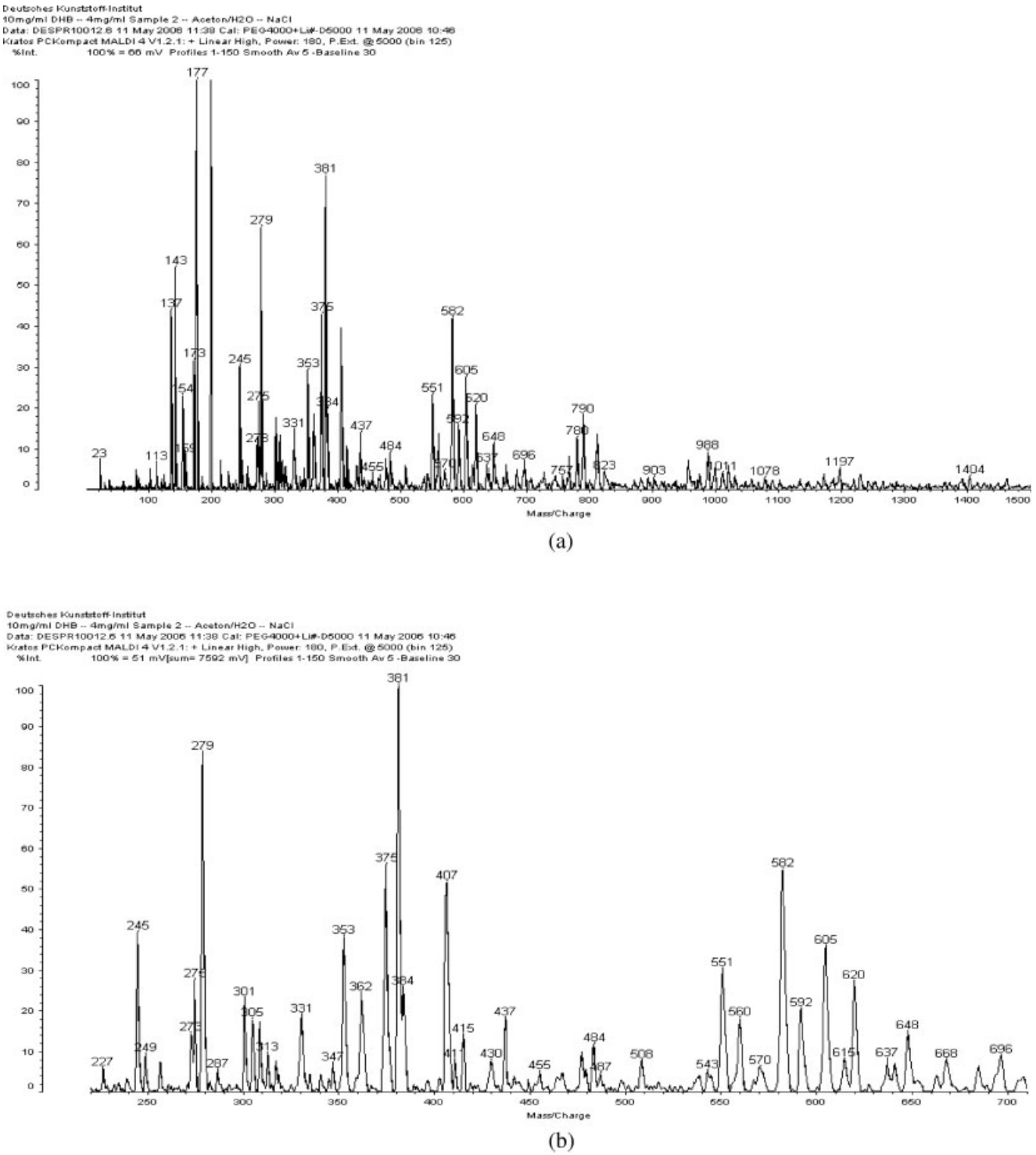

Figure 3 MALDI-TOF spectra of MUF sample 2: (a) the 1–1500-Da region and (b) a detail of the 220–710-Da region.

for a number of transients (ca. 1000). All the spectra were run with a relaxation delay of 5 s, and the chemical shifts were accurate to 1 ppm.

DISCUSSION

The multistage MUF resin was manufactured according to an industrial formulation with just one variation, this being an important one. In industrial urea–formaldehyde (UF) and MUF formulations, the UF condensation stage is performed at a pH between 5 and 6. In our case, the pH was kept relatively high at 7.8. This was done first to considerably slow down the reaction and second to check that (1) at this pH UF oligomers could be formed just by the

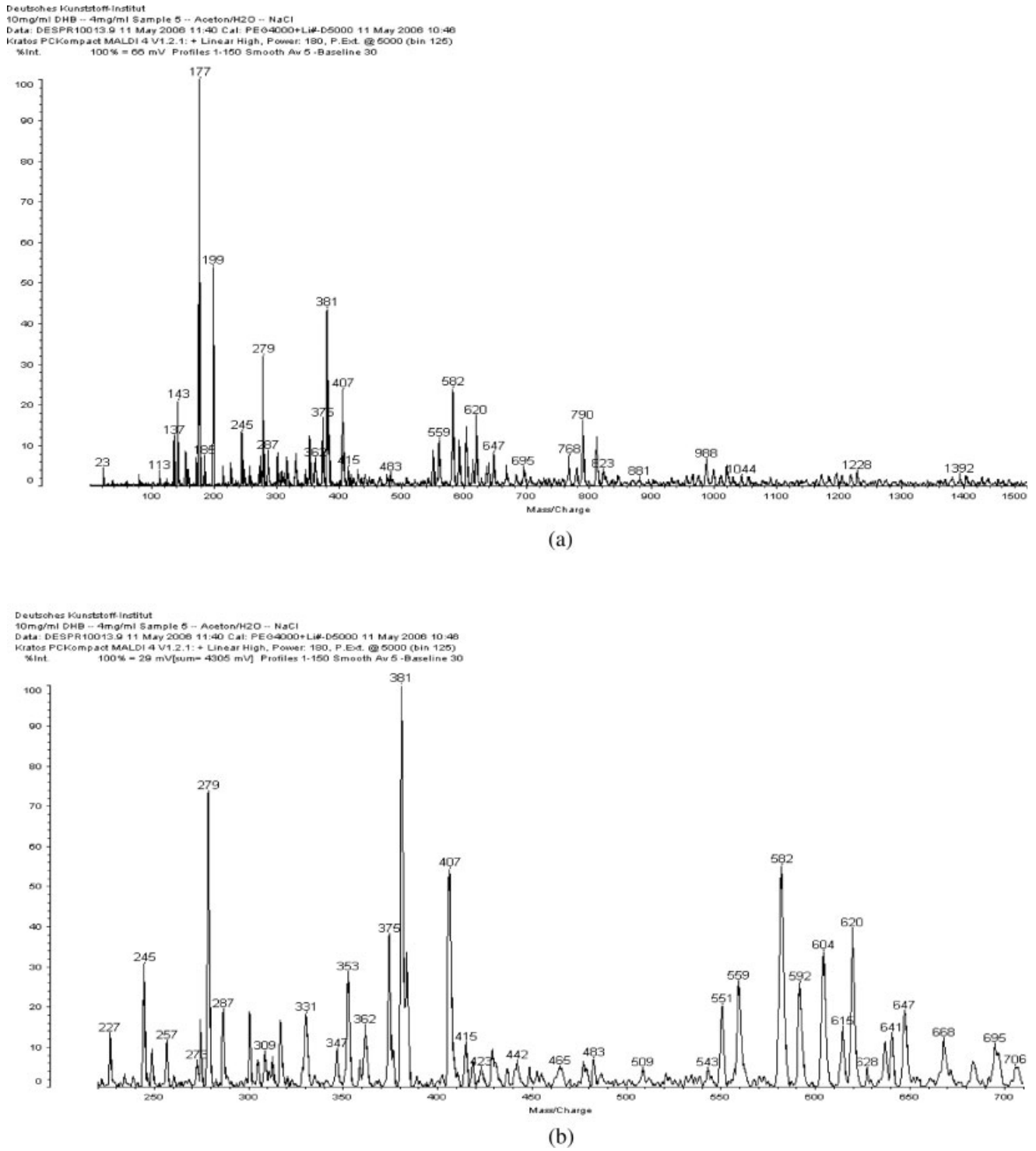

Figure 4 MALDI-TOF spectra of MUF sample 5: (a) the 1–1500-Da region and (b) a detail of the 220–710-Da region.

joining of the ureas by methylene ether bridges, (2) the rearrangement to methylene bridges could be induced by the addition of melamine at the same pH by a coreaction with the preformed UF condensate, (3) alternatively methylene bridges could form also at a very alkaline pH as the condensation reaction properly starts only at pHs less than 8, and (4) a relatively high proportion of methylene ether bridges could be carried over also to the end of the reaction after melamine addition.

The classical theory of UF polycondensation states that at a very alkaline pH, only methylol groups (—CH_2OH) and methylene ether bridges (—CH_2OCH_2—) between ureas form, the latter lead-

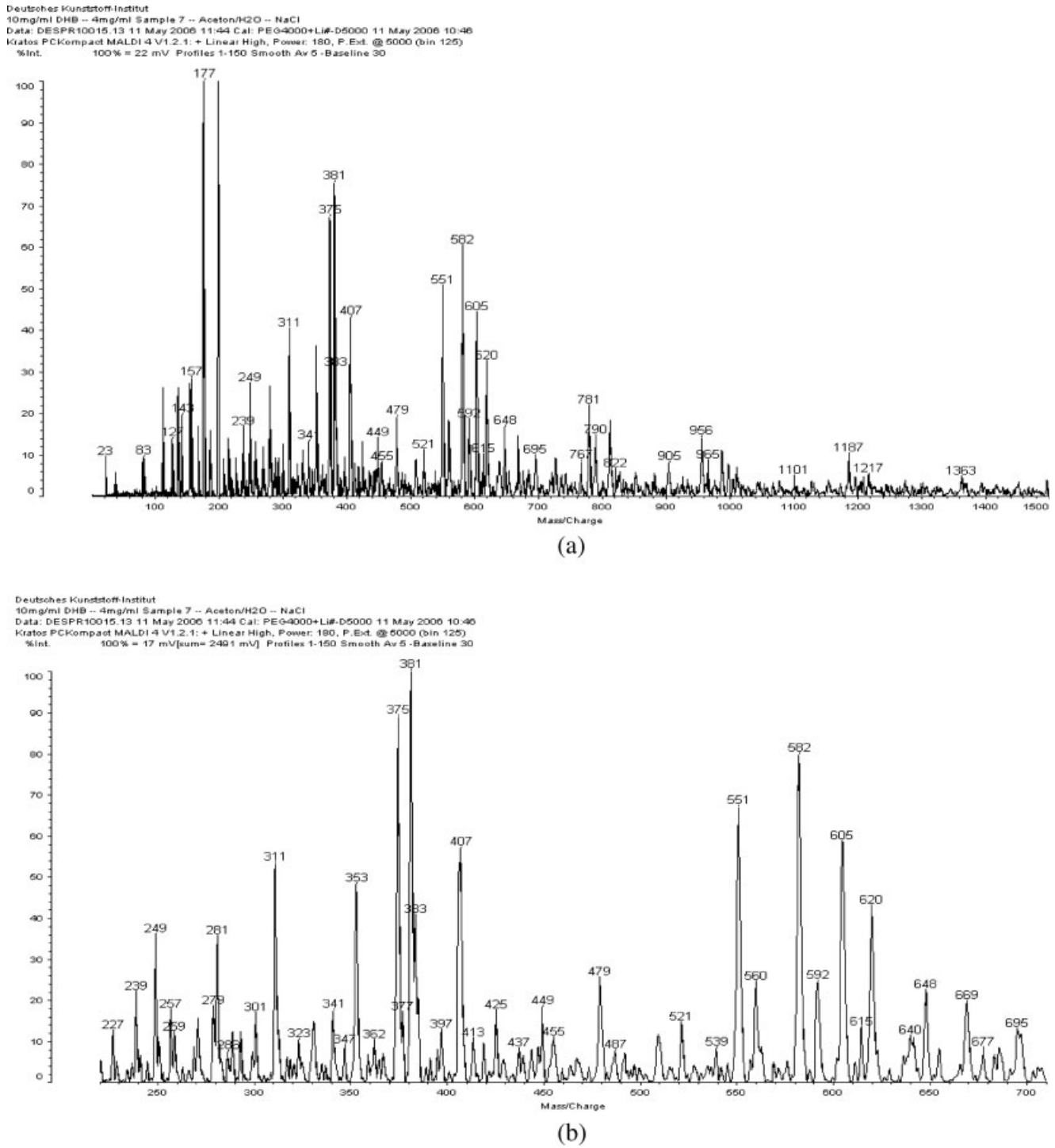

Figure 5 MALDI-TOF spectra of MUF sample 7: (a) the 1–1500-Da region and (b) a detail of the 220–710-Da region.

ing only to very short oligomers.[8,9] No methylene bridges (—CH_2—) between ureas are supposed to be formed at a very alkaline pH.

Figure 1 shows the course of the temperature and pH during the reaction. The different phases of resin manufacture are also shown: the first phase is the building of the UF resin skeleton, the second phase is the condensation of melamine on the methylol groups of the UF resin to form the MUF cocondensate, and the third phase is the addition of the final urea to mop up any excess free formaldehyde. The same figure shows at which point in the preparation the samples were collected: (1) at the beginning of the UF reaction, (2) when a temperature of 90°C and a lower pH for the polycondensation part of the UF reaction were reached, (5) at the end of the polycon-

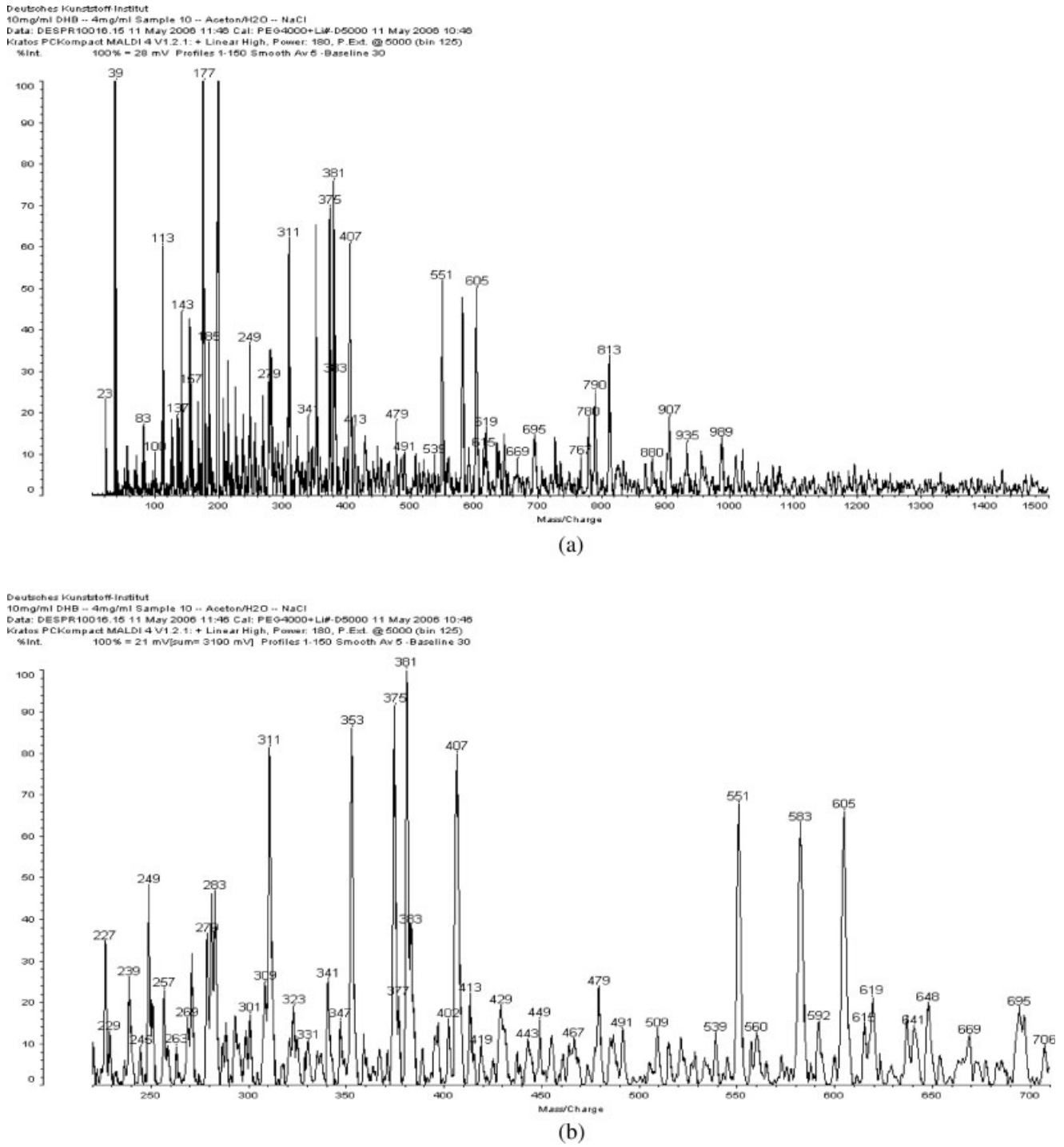

Figure 6 MALDI-TOF spectra of MUF sample 10: (a) the 1–1500-Da region and (b) a detail of the 220–710-Da region.

densation part of the UF reaction before melamine addition, (7) 10 min after melamine addition, (10) well into the condensation reaction of melamine with UF to give the MUF cocondensates, (12) upon the addition of the second and last urea for mopping up formaldehyde and a pH increase to slow the condensation down, and (14) at the end of the reaction after cooling.

Figures 2–7 show the MALDI-TOF mass spectra, and Tables I–IV show the species present in the first half of the reaction before and after the melamine addition. The relative abundance distribution of the species is shown in Figures 2–7.

Tables I and II report two alternative interpretations of the MALDI-TOF results with respect to all the species present at the beginning of the UF poly-

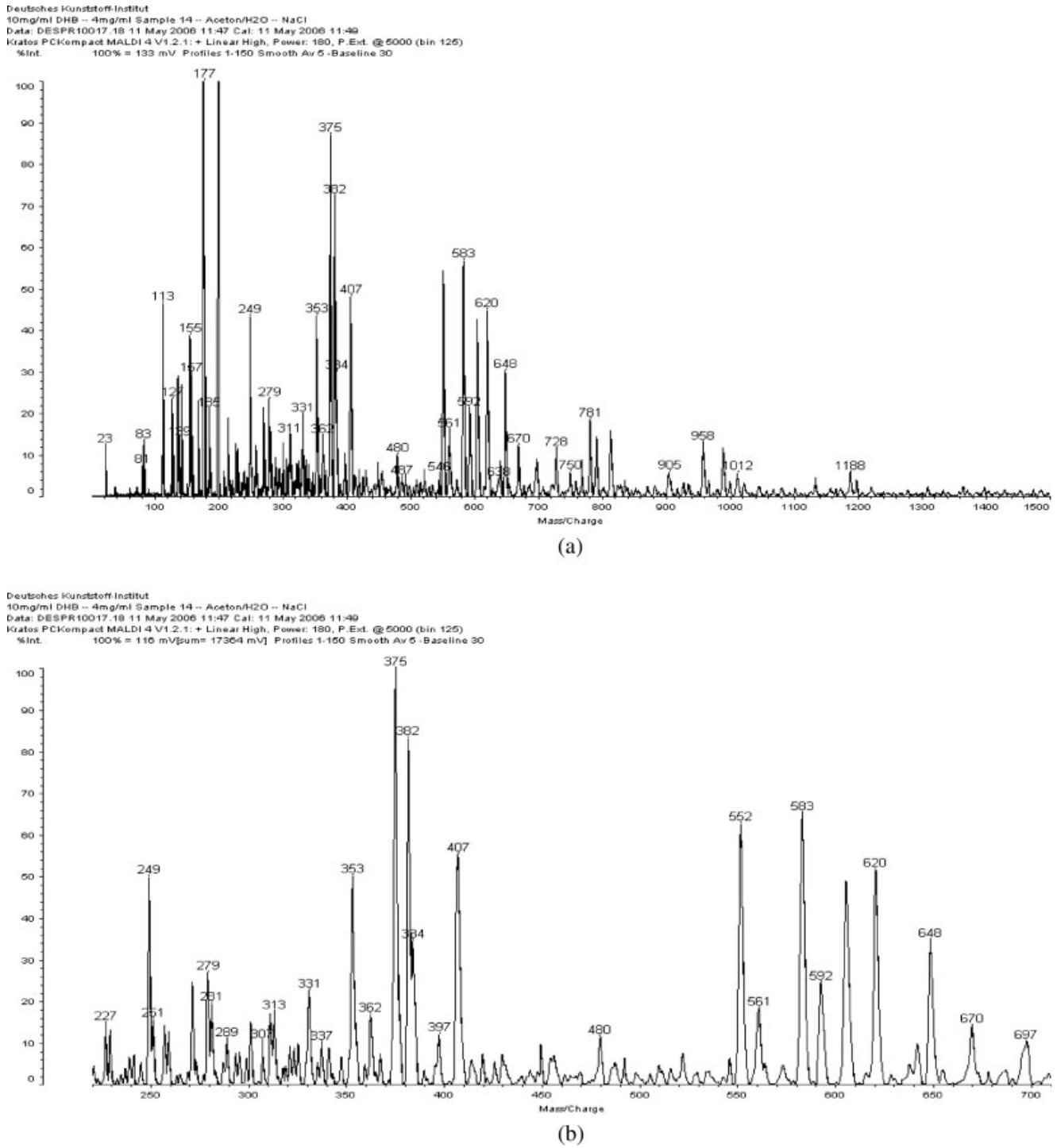

Figure 7 MALDI-TOF spectra of MUF sample 14: (a) the 1–1500-Da region and (b) a detail of the 220–710-Da region.

condensation stage of urea and formaldehyde to form UF oligomers. The polycondensation phase starts, although slowly, before sample 2 is taken (reported in Tables I and II) but later than sample 1, as soon as the pH starts to dip. Furthermore, the UF condensation phase is maintained at a pH much higher than is usually the case, as explained previously. This is done to slow down and better control the reaction so that the successive samples can be taken at well-defined stages of the reaction without the reaction proceeding too fast and altering the condition of the samples. Tables I and II and Figures 2 and 3 show that the molecular weights of the species present are the same. This might not mean that the species present are the same because at the beginning of the reaction (sample 1), when the

TABLE I
MALDI-TOF Fragmentation Peaks of Sample 2: The Distribution of the Structures If the Reaction Were Carried Out at a Lower pH As Forecast by the Classical Theory of UF Resin Formation

Experimental M + Na^+ (Da)	Chemical species
23	Na
113 (112[a])	U—CH_2OH
137	
143 (141[a])	$HOCH_2$—U—CH_2OH
154	U—CH_2—U
177 (170[a])	$HOCH_2$—U—$(CH_2OH)_2$ (100% peak)
199	$^+CH_2$—U—CH_2—U—CH_2OH (or CH_2—U—CH_2—O—CH_2—U in the beginning of the reaction)
227	U—CH_2—U—CH_2—U (very small proportion)
245	$HOCH_2$—U—CH_2—U—$(CH_2OH)_2$ (or $HOCH_2$—U—CH_2—O—CH_2—U—CH_2OH in the beginning of the reaction)
275	$(HOCH_2)_2$—U—CH_2—U—$(CH_2OH)_2$ [or $(HOCH_2)_2$—U—CH_2—O—CH_2—U—CH_2OH in the beginning of the reaction]
279	Like 275 but tetraprotonated
301	$^+CH_2$—U(—CH_2OH)—CH_2—U—CH_2—U—CH_2OH [119 + —CH_2—U(—CH_2OH)—] and 119 alternative
331	CH_2—U(—CH_2OH)—CH_2—U—CH_2—U—$(CH_2OH)_2$ (301 + —CH_2OH) and 301 alternative
353	$(HOCH_2)_2$—U—CH_2—U—(CH_2OH)—CH_2—U—CH_2OH
362	U—CH_2—U—[CH_2—U(—CH_2OH)—CH_2—U—(CH_2OH)]—H
375	$(HOCH_2)_2$—U—CH_2—U(—CH_2OH)—CH_2—U—$(CH_2OH)_2$
381	$(HOCH_2)_2$—U—CH_2—U(—CH_2OH)—CH_2—U—$(CH_2OH)_2$ tetraprotonated
484	$(HOCH_2)_2$—U—CH_2[—U(—CH_2OH)—CH_2]$_2$—U—$(CH_2OH)_2$ tetraprotonated
551	$(HOCH_2)_2$—U—CH_2—U—CH_2[—U(—CH_2OH)—CH_2]$_3$—OH
570	U—CH_2—U—[CH_2—U(—CH_2OH)—CH_2—U—(CH_2OH)]$_2$—H
582	$(HOCH_2)_2$—U—CH_2[—U(—CH_2OH)—CH_2]$_3$—U—$(CH_2OH)_2$
605	$(HOCH_2)_2$—U—CH_2—[U(CH_2^+)(—CH_2OH)—CH_2—][—U(—CH_2OH)—CH_2]$_2$—U—$(CH_2OH)_2$
620	$(HOCH_2)_2$—U—CH_2—[U(CH_2^+)(—CH_2OH)—CH_2—]$_2$—[—U(—CH_2OH)—CH_2]—U—$(CH_2OH)_2$
780	U—CH_2—U—[CH_2—U(—CH_2OH)—CH_2—U—(CH_2OH)]$_3$—H
790	$(HOCH_2)_2$—U—CH_2[—U(—CH_2OH)—CH_2—] [—U(—CH_2OH)—CH_2—U—(CH_2OH)— CH_2]$_2$—U—$(CH_2OH)_2$
988	U—CH_2—U—[CH_2—U(—CH_2OH)—CH_2—U—(CH_2OH)]$_4$—H
1078	$(HOCH_2)_2$—U—CH_2—U(—CH_2OH)—[CH_2—U(—CH_2OH)—CH_2—U—(CH_2OH)]$_4$—H
1197	U—CH_2—U—[CH_2—U(—CH_2OH)—CH_2—U—(CH_2OH)]$_5$—H
1404	U—CH_2—U—[CH_2—U(—CH_2OH)—CH_2—U—(CH_2OH)]$_6$—H

In the case of sample 1, any U—(CH_2OH)—CH_2—U group could be instead —U—CH_2O—CH_2—U—. U = urea.
[a] Calculated.

pH is still very alkaline, methylene ether bridges (—CH_2OCH_2—) should definitely abound. These reorganize during condensation at a lower pH to methylene bridges (—CH_2—), with an emission of formaldehyde reacting again with urea or a UF oligomer to form at first a methylol group (—CH_2OH). The molecular weights of samples of formulas U—CH_2OCH_2—U and U(—CH_2OH)—CH_2—U are the same; thus, the two types of structures cannot be distinguished just by MALDI-TOF. As it is known that at a very alkaline pH methylene ether bridges (—CH_2OCH_2—) do form and methylene bridges (—CH_2—) do not, the assignment of the peaks in Table I for the same molecular weight must take into account this point. Thus, for example, the peak at 245 Da could be either $HOCH_2$—U—CH_2OCH_2—U—CH_2OH, as is surely the case for sample 1 in Figure 2 because the literature shows that no methylene bridges occur at this pH, or just $HOCH_2$—U—CH_2—U—$(CH_2OH)_2$ for sample 2 (Fig. 3 and Table II) or a mix of the two species. This at least should be the interpretation of the MALDI-TOF results according to the classic theory of UF resin formation. This, however, does not appear to be totally the case because short oligomers in which the methylol group (—CH_2OH) is not present occur both in Figure 2 and in Figure 3. Thus, a small number of methylene bridges (—CH_2—) between ureas do form even at pHs higher than what is foreseen by the classic theory of UF resin formation. For instance, the small peaks at 154–155 and 227 Da belong, respectively and exclusively, to U—CH_2—U and U—CH_2—U—CH_2—U. This means that methylene bridges do indeed form also at very alkaline pHs; they are only much less frequent. It is not possible to ascertain this for higher molecular weight oligomers as they are all methylolated and one cannot distinguish between U—CH_2OCH_2—U and U(—CH_2OH)—CH_2—U species for sample 1 or hence determine which of the two exist, and if both exist, in what proportions.

To determine if the real structures existing are those reported in Table I or those reported in Table II, the difference in the structures needs to be examined by ^{13}C-NMR of the same samples (samples 1

TABLE II
MALDI-TOF Fragmentation Peaks of Sample 2: The Real Distribution of the Structures After Confirmation by ^{13}C-NMR

Experimental M + Na^+ (Da)	Chemical species
23	Na
113 (112[a])	U—CH_2OH
137	
143 (141[a])	$HOCH_2$—U—CH_2OH
154	U—CH_2—U
177 (170[a])	$HOCH_2$—U—$(CH_2OH)_2$ (100% peak)
199	$^+CH_2$—U—CH_2—O—CH_2—U (or $^+CH_2$—U—CH_2—U—CH_2OH if the pH had to be much lower)[b]
227	U—CH_2—U—CH_2—U (very small proportion)
245	$HOCH_2$—U—CH_2—O—CH_2—U—CH_2OH [or $HOCH_2$—U—CH_2—U—$(CH_2OH)_2$ in a more acidic reaction][b]
275	$(HOCH_2)_2$—U—CH_2—O—CH_2—U—CH_2OH [or $(HOCH_2)_2$—U—CH_2—U—$(CH_2OH)_2$ in a more acidic reaction][b]
279	Like 275 but tetraprotonated
301	$^+CH_2$—U—CH_2OCH_2—U—CH_2OCH_2—U (119 + —CH_2OCH_2—U—) and 119 alternative[b]
332	$^+CH_2$—U—CH_2OCH_2—U—CH_2OCH_2—U—CH_2OH (301 + —CH_2OH) and 301 alternative[b]
353	$HOCH_2$—U—CH_2OCH_2—U—CH_2OCH_2—U—CH_2OH
362	U—CH_2—U—[CH_2—U—CH_2OCH_2—U—(CH_2OH)]—H
375	$HOCH_2$—U—CH_2OCH_2—U—CH_2OCH_2—U—$(CH_2OH)_2$
381	$HOCH_2$—U—CH_2OCH_2—U—CH_2OCH_2—U—$(CH_2OH)_2$ tetraprotonated
484	$HOCH_2$—U—CH_2OCH_2—[—U—CH_2OCH_2]$_2$—U—$(CH_2OH)_2$ tetraprotonated
551	$HOCH_2$—U—CH_2OCH_2—U—CH_2[—OCH_2—U—CH_2]$_3$—OH
570	U—CH_2—U—[—CH_2OCH_2—U—CH_2OCH_2—U]$_2$—H
582	$(HOCH_2)_2$—U—CH_2[—OCH_2—U—CH_2]$_3$—OCH_2—U—CH_2OH
605	$(HOCH_2)_2$—U—CH_2—[OCH_2—U(CH_2^+)—CH_2—][—OCH_2—U—CH_2]$_2$—OCH_2—U—CH_2OH
620	$(HOCH_2)_2$—U—CH_2—[OCH_2—U(CH_2^+)—CH_2—]$_2$—[—OCH_2—U—CH_2]—OCH_2—U—CH_2OH
780	U—CH_2—U—[—CH_2OCH_2—U—CH_2OCH_2—U]$_3$—H
790	$(HOCH_2)_2$—U—CH_2[—OCH_2—U—CH_2—] [—OCH_2—U—CH_2OCH_2—U—CH_2—]$_2$—OCH_2—U—CH_2OH
988	U—CH_2—U—[—CH_2OCH_2—U—CH_2OCH_2—U]$_4$—H
1078	$HOCH_2$—U—CH_2OCH_2—U—[—CH_2OCH_2—U—CH_2OCH_2—U]$_4$—CH_2OH
1197	U—CH_2—U—[—CH_2OCH_2—U—CH_2OCH_2—U]$_5$—H
1404	U—CH_2—U—[—CH_2OCH_2—U—CH_2OCH_2—U]$_6$—H

In the case of sample 1, any U—(CH_2OH)—CH_2—U group could instead be —U—CH_2O—CH_2—U—. U = urea.
[a] Calculated.
[b] All higher oligomers would follow this pattern too if the reaction were performed at a much lower pH.

and 2; Figs. 8 and 10). Figures 8(a) and 10(a) for samples 1 and 2 show four peaks, none of which corresponds to that of unreacted urea (162.5 ppm; Fig. 9). The four peaks correspond to trisubstituted urea (158.6 ppm) and *N,N′*-disubstituted urea (159.1 ppm). The 160.7 ppm peak corresponds to monosubstituted urea, and the 160.2 ppm corresponds to the *N,N*-disubstituted urea. Even more indicative is the series of bands in the 40–90 ppm range [Figs. 8(b) and 10(b)]. All the peaks in this range belong to methylol groups (—CH_2OH) or to methylene ether bridges, as indicated in the figure itself. There is no trace of methylene bridges (which should appear at 45–47 ppm). Figures 8(b) and 10(b) confirm that the MALDI peaks of samples 1 and 2 and up to sample 7 do not contain any major amount of methylene bridges, confirming that the structures shown in Table II are the correct interpretation of the data. The amount is so low that is undetectable by NMR, and MALDI indicates only very low proportions of them. There are almost exclusively methylene ether bridges and methylol groups, without any methylene bridges being present. Even more important, the first noticeable number of methylene bridges starts to appear only with sample 10 (shown later in Fig. 13), and they are either melamine-to-melamine bridges or melamine-to-urea bridges. Alternatively, if they are urea-to-urea bridges, they imply that melamine induces the rearrangement of methylene ether bridges between ureas to form urea-to-urea methylene bridges. In Figure 13 (shown later), the integral indicates for the first time an important proportion of methylene and methylene ether bridges, but the latter are still predominant by far. The absence of methylene bridges in the purely UF preparation phase (Table II and Figs. 8 and 10–12) can be explained by the rather high pH of the polycondensation chosen. This is too high to allow UF condensation to properly proceed to the formation of methylene bridges. Thus, the formulas of the compounds in Table I must be interpreted as in Table II and hence as a function of rather long oligomers being

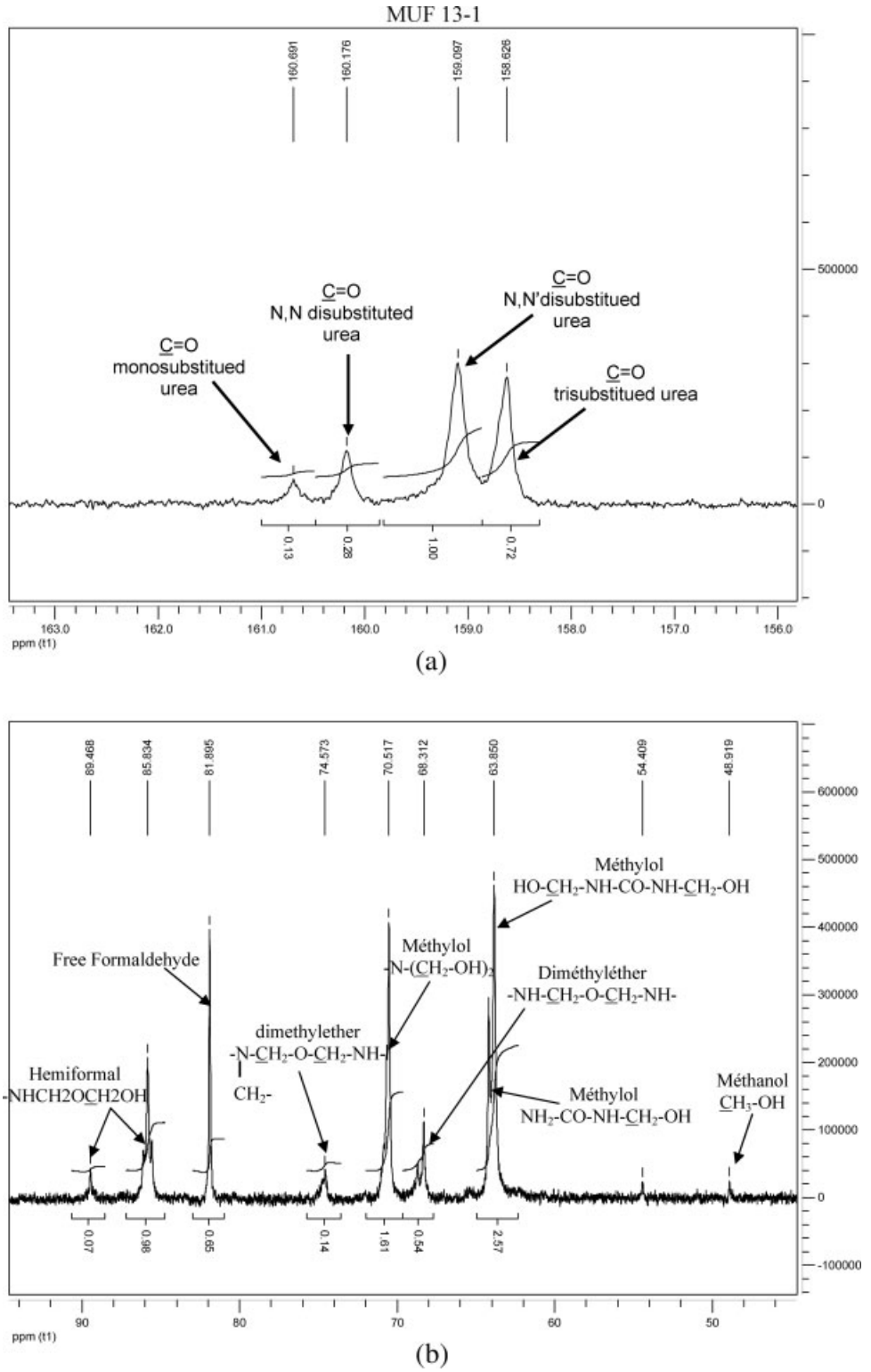

Figure 8 ^{13}C-NMR spectra of sample 1: (a) a detail of the 150–170 ppm region and (b) a detail of the 43–85 ppm region.

present that are formed in a great majority by methylol-to-methylol condensation to form methylene ether bridges. Thus, the species listed in Table II are the ones really present under the particular reaction conditions under which the experiment was carried out. These structures, once formed, must be considered still relatively stable and able to tolerate the insertion of melamine while maintaining to a high degree the methylene ether oligomer structure. The formation of methylene bridges appears, however, to

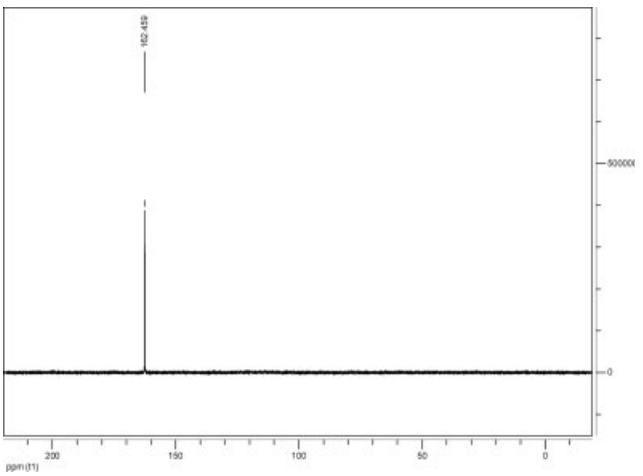

Figure 9 ^{13}C-NMR spectrum of urea in water at a 40% concentration.

be accelerated by the introduction of the melamine. The rearrangement to urea-to-urea methylene bridges of the methylene ethers during the melamine part of the reaction is possibly facilitated by the long heating times necessary to perform the reaction under the relatively higher alkalinity conditions used.

In the case of sample 7 (Table III), the NMR spectra indicate that $—CH_2OCH_2—$ is the totality of the bridges existing. Methylene bridges are in such a small proportion that they cannot even be detected by NMR, notwithstanding the fact that the MALDI-TOF analysis clearly indicates that species containing small proportions of them are clearly present. In the case of sample 14 (Table IV) at the end of the reaction, the NMR analysis clearly detects a noticeable percentage of methylene bridges, these being mixed with a predominant percentage of methylene ether ($—CH_2OCH_2—$) bridges.

Table V presents the progression of the relative abundance of some of the MF and MUF chemical species. The species of type $(HOCH_2—)_3—M—(—CH_2—U—)_2—H$ and thus methylolated MUF oligomers (381 Da) are proportionally the most abundant from the start of the addition of melamine to the reaction mixture. These species are most likely derived from a reaction of melamine with free formaldehyde in the reaction mixture that forms methylol melamines and by a simultaneous reaction with methylol urea monomers and dimers and methylene ureas (e.g., the species at 113, 143, and 154 Da).

In sample 2 (Fig. 10 and Table II), the primary pattern of relative species abundance is 177, 279, 381, 484, and 582 Da (Table II). The heavily methylolated multimethylene urea oligomers with the 177-, 381-, and 587-Da pattern remain more abundant also in sample 7, but with other important patterns appearing too at this stage of the reaction. By the end of the preparation, for sample 14, to this same pattern one of equal importance has been added, namely, the one with similar peaks based on the reaction of the UF resin with melamine to form the MUF oligomers.

As the reaction proceeds and one passes from sample 7 to sample 14, the relative proportion of methylolation of the melamine starts to increase, from the trimethylolated species being in a higher proportion in sample 7 to the tetramethylolated species in sample 10, and then decreases in sample 14. The same trend is observed when the reaction of the melamine is not only with formaldehyde but also with the methylol urea monomers and dimer. Thus, for example, the 311-Da species proportion increases from sample 7 to sample 10, at which it reaches its maximum proportion, and finally decreases in sample 14. However, tetrareacted melamine is still in the highest proportion, and for the commercial MUF formulation used, melamine species more than tetrareacted do not occur. This appears valid for the reaction of the melamine both with formaldehyde and with methylol ureas. After tetrasubstitution, the chain appears to grow linearly as a side chain.

Following the reaction by ^{13}C-NMR, we can observe a few trends. Thus, from sample 1 to sample 2, the proportion of $HOCH_2—U—CH_2OH$ (63.85 ppm) increases, and that of monomethylolated ureas ($U—CH_2OH$; 64 ppm) decreases as the UF reaction progresses [Figs. 8(b) and 10(b)]. Equally, the relative proportion of methylene ether bridges (68.2 and 74.5 ppm) increases, free formaldehyde (81.9 ppm) decreases, and hemiformals decrease [Figs. 8(b) and 10(b)]. Some uron (154 ppm) and methylol groups of uron (77.8 ppm) start to appear in sample 2 (Figs. 8 and 10). All these trends continue further in sample 5.

The pattern changes with sample 7 immediately after melamine is added (Fig. 12). Thus, the $—CH_2OH$ band of methylolated melamine at 64.1 ppm appears almost as strong as that of *N,N′*-disubstituted urea, whereas that of monosubstituted urea has become even lower. The relative proportion of methylene ether bridges increases sharply, as shown by the series of bands between 66.9 and 68 ppm [Fig. 12(b)]. Even more characteristic changes can be noted downfield in the higher parts per million region. Here the peaks of unreacted, monoreacted, direacted, and multireacted melamines (Fig. 12) at 166.16 and 165.3 ppm clearly appear, as does a pattern of C=O of unsubstituted (162.2 ppm), monosubstituted (160.5 ppm), disubstituted, and multisubstituted ureas (*N,N* at 160.04 ppm and *N,N′* at 158.9 ppm) in line with what is deduced by MALDI-TOF, as shown in Table III. The signal of urons and substituted urons take the same characteristic three-peak configuration as urea, these appearing at 155.6, 154.6, and 153.9–154 ppm, respectively (Fig. 12).

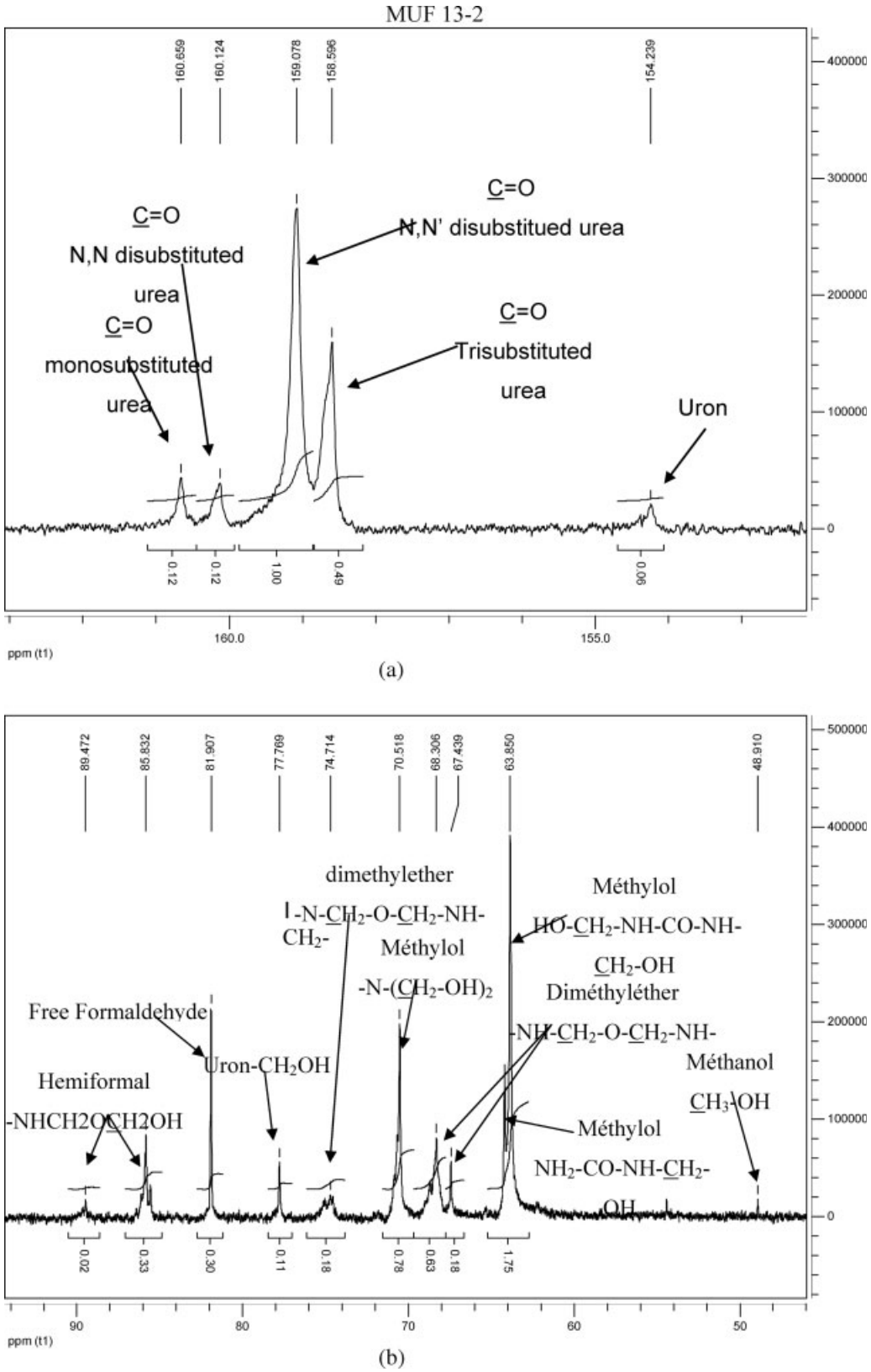

Figure 10 ^{13}C-NMR spectra of sample 2: (a) a detail of the 150–170 ppm region and (b) a detail of the 43–85 ppm region.

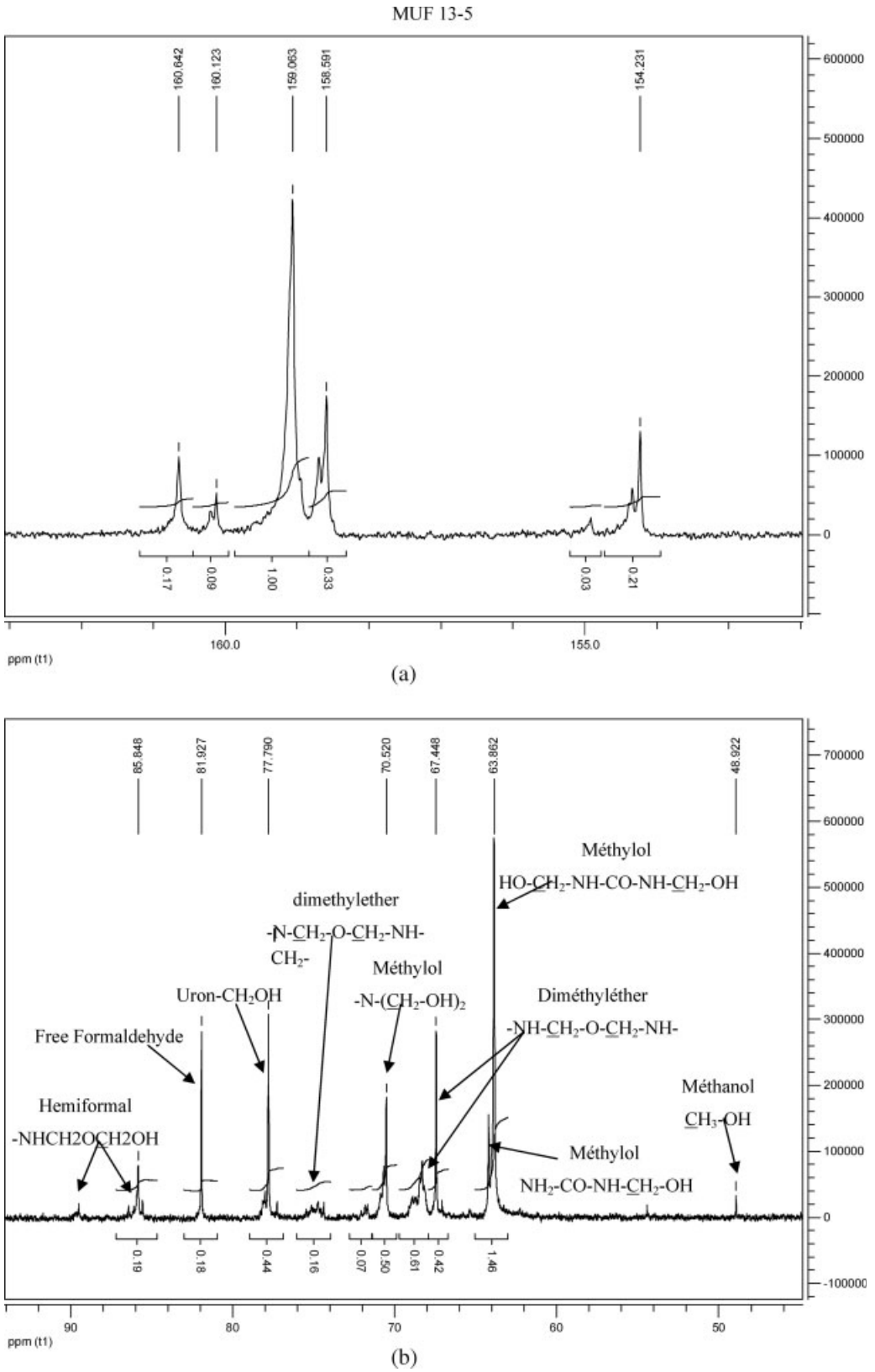

Figure 11 ^{13}C-NMR spectra of sample 5: (a) a detail of the 150–170 ppm region and (b) a detail of the 43–85 ppm region.

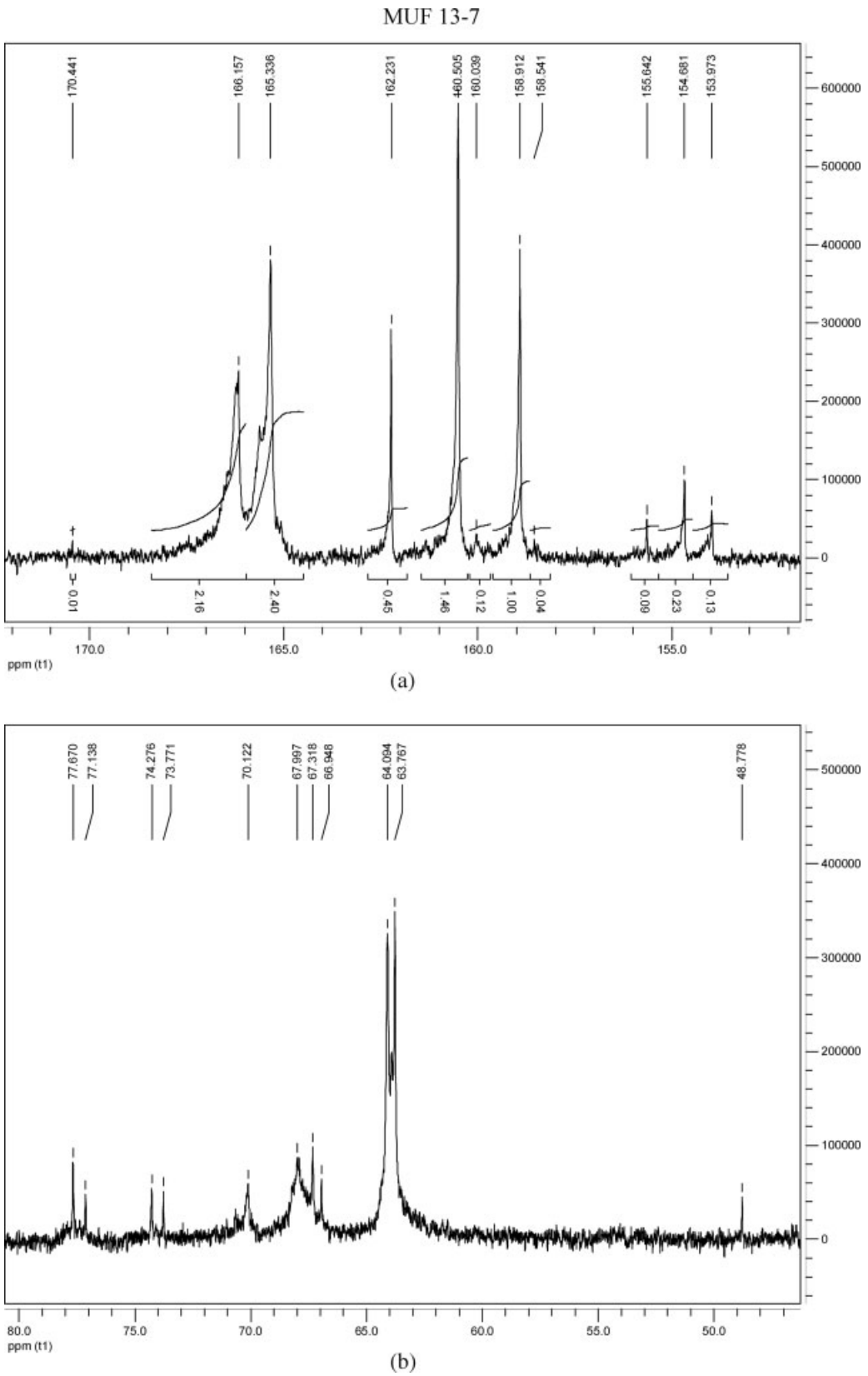

Figure 12 ^{13}C-NMR spectra of sample 7: (a) a detail of the 150–170 ppm region and (b) a detail of the 43–85 ppm region.

TABLE III
MALDI-TOF Fragmentation Peaks of Sample 7

Experimental M + Na^+ (Da)	Chemical species
127	$^+CH_2-U-CH_2OH$
143 (141[a])	$HOCH_2-U-CH_2OH$
157 (154[a])	$U-CH_2-U$
177	$\boldsymbol{M}-CH_2OH$
199	$^+CH_2-U-CH_2-U-CH_2OH + 2H^+$ protonated (or $^+CH_2-U-CH_2OCH_2-U$ at 197 Da)
209	$\boldsymbol{M}-(CH_2OH)_2$
239 (237[a])	$\boldsymbol{M}-(CH_2OH)_3$
249 (245[a])	$HOCH_2-U-CH_2OCH_2-U-CH_2OH$ [possibly in later samples $HOCH_2-U-CH_2-U-(CH_2OH)_2$]
270	$(HOCH_2)_2-\boldsymbol{M}-(CH_2OH)_2$
279–281[b]	$U-CH_2-U-CH_2-U-CH_2OH$ and $U-CH_2-U-CH_2OCH_2-U$
311	$U-CH_2-\boldsymbol{M}-(CH_2OH)_3$
353	Mainly $HOCH_2-U-CH_2OCH_2-U-CH_2OCH_2-U-CH_2OH$
375 (371[a])	$\boldsymbol{M}-CH_2-U-CH_2-\boldsymbol{M}=CH_2 + 4H^+$
381 (383[a])	$H-(U-CH_2)_2-\boldsymbol{M}-(CH_2OH)_3$
407	$HOCH_2-\boldsymbol{M}-CH_2-U-CH_2-\boldsymbol{M}=CH_2 + 4H^+$ protonated
425	$U-CH_2-U-CH_2-U-(CH_2OH)-[-CH_2-U-]_2H$ and $U-CH_2-U-CH_2-U-CH_2O-[-CH_2-U-]_2H$
455	$H-(U-CH_2)_3-\boldsymbol{M}-(CH_2OH)_3$
551[b]	$CH_2=\boldsymbol{M}-CH_2UCH_2-\boldsymbol{M}-CH_2UCH_2-U-CH_2OH$
582[b]	Same species as sample 2 (Table II) and $CH_2=\boldsymbol{M}-CH_2UCH_2-\boldsymbol{M}(-CH_2OH)-CH_2UCH_2-U-CH_2OH$ and $CH_2=\boldsymbol{M}-CH_2UCH_2-\boldsymbol{M}(-CH_2OH)-CH_2U-CH_2OCH_2-U$
767	
782 (784[a])	$CH_2=\boldsymbol{M}-CH_2UCH_2-\boldsymbol{M}(-CH_2OH)-CH_2UCH_2-[U(-CH_2OH)-CH_2]_2-U-CH_2OH$ and $CH_2=\boldsymbol{M}-CH_2UCH_2-\boldsymbol{M}(-CH_2OH)-CH_2UCH_2-[U-CH_2OCH_2-]_2-U-CH_2OH$
790[b]	Like Table II and $(HOCH_2)_3-\boldsymbol{M}-CH_2-U(-CH_2OH)-CH_2-[U-CH_2]_2-\boldsymbol{M}-(CH_2OH)_3$ and/or $(HOCH_2)_3-\boldsymbol{M}-CH_2-U-CH_2OCH_2-[U-CH_2]_2-\boldsymbol{M}-(CH_2OH)_3$ and/or $(HOCH_2)_2-\boldsymbol{M}-CH_2-U-CH_2OCH_2-[U-CH_2OCH_2]_2-\boldsymbol{M}-(CH_2OH)_2$
822 (820[a])	Mainly $(HOCH_2)_3-\boldsymbol{M}-CH_2-U-CH_2OCH_2-U-CH_2OCH_2-U-CH_2-\boldsymbol{M}-(CH_2OH)_3$ and/or $(HOCH_2)_3-\boldsymbol{M}-CH_2-U(-CH_2OH)-CH_2-U(-CH_2O)-CH_2-U-CH_2-\boldsymbol{M}-(CH_2OH)_3$
956	Mainly $CH_2=\boldsymbol{M}-(CH_2OH)_2-CH_2UCH_2-\boldsymbol{M}(=CH_2)(CH_2OH)-CH_2UCH_2-[U-CH_2OCH_2]_3-U-CH_2OH$ and/or $CH_2=\boldsymbol{M}-(CH_2OH)_2-CH_2UCH_2-\boldsymbol{M}(=CH_2)(CH_2OH)-CH_2UCH_2-[U(-CH_2OH)-CH_2]_3-U-CH_2OH$
1187	Mainly $CH_2=\boldsymbol{M}-(CH_2OH)_2-CH_2UCH_2-\boldsymbol{M}(=CH_2)(CH_2OH)-CH_2UCH_2-[U-CH_2OCH_2]_5-U-(CH_2OH)_2$ and/or $CH_2=\boldsymbol{M}-(CH_2OH)_2-CH_2UCH_2-\boldsymbol{M}(=CH_2)(CH_2OH)-CH_2UCH_2-[U(-CH_2OH)-CH_2]_5-U-(CH_2OH)_2$ equivalent to 2M + 8U and/or 6M + 3U and/or $HOCH_2-U-CH_2UCH_2-\boldsymbol{M}(-CH_2OH)-CH_2UCH_2-\boldsymbol{M}(-CH_2OH)-CH_2-[-\boldsymbol{M}-CH_2-]_3-\boldsymbol{M}=CH_2$
1217	1187 + $1x-CH_2OH$ more
1363	1187 + $1x(-U-CH_2-)_2$ and + $1x-CH_2OH$ more

Urea-to-urea methylene ethers structures still predominate in sample 7. ^{13}C-NMR indicates the very predominant presence of methylol groups and urea-to-urea methylene ether bridges but also practically the absence of methylene bridges. U = urea.

[a] Calculated.

[b] There may be different species of the same peak in Table I mixed with the melamine species shown in this table.

As the reaction proceeds after the addition of melamine to the UF resin (sample 10; Fig. 13), methylene bridges start to appear, the *N,N′*-disubstituted urea peak at 160.5 ppm becomes more prominent, and multisubstituted melamine peaks appear and become progressively more prominent too, the substituted main peak resolving itself into shoulders of multisubstituted melamine. The melamine peaks widen and thin as well from sample 10 to sample 14 through samples 11 and 12 (Figs. 13–16). This indicates that in this phase the reaction proceeds as a sequel to steady-state conditions caused by slowly changing dynamic equilibria. The reaction mixture goes through a phase in which the same compounds form and decrease and then increase again, giving the impression of overall stability in the relative proportions of the compounds. This slowly changing state, in appearance a steady state, is however the result of considerable dynamic movement and shifting equilibria. For example, the proportion of urons, as shown by the three C=O peaks at 153–156 ppm, remains at first stable (from sample 10 to sample 11 and then sample 12; Figs. 13–15) and then decreases (samples 7–14; Figs. 12–16), indicating their conversion to reacted urea.

The already low level of free formaldehyde decreases [from sample 10 to sample 11; Figs. 13(b) and 14(b)], and then formaldehyde disappears [from

TABLE IV
MALDI-TOF Fragmentation Peaks of Sample 14

Experimental M + Na^+ (Da)	Chemical species
127	$^+CH_2$—U—CH_2OH
157 (154[a])	U—CH_2—U
177	***M***—CH_2OH
199	$^+CH_2$—U—CH_2—U—CH_2OH + $2H^+$ protonated (or $^+CH_2$—U—CH_2OCH_2—U at 197 Da)
209	***M***—$(CH_2OH)_2$
239 (237[a])	***M***—$(CH_2OH)_3$
249 (245[a])	$HOCH_2$—U—CH_2OCH_2—U—CH_2OH [possibly in later samples $HOCH_2$—U—CH_2—U—$(CH_2OH)_2$]
270	$(HOCH_2)_2$—***M***—$(CH_2OH)_2$
279–281[b]	U—CH_2—U—CH_2—U—CH_2OH and U—CH_2—U—CH_2OCH_2—U
311	U—CH_2—***M***—$(CH_2OH)_3$
353	Mainly $HOCH_2$—U—CH_2OCH_2—U—CH_2OCH_2—U—CH_2OH
375 (371[a])	***M***—CH_2—U—CH_2—***M***=CH_2 + $4H^+$
381 (383[a])	H—[U—CH_2]$_2$—***M***—$(CH_2OH)_3$
407	$HOCH_2$—***M***—CH_2—U—CH_2—***M***=CH_2 + $4H^+$ protonated
455	H—$(U—CH_2)_3$—***M***—$(CH_2OH)_3$
546	$HOCH_2$—U—CH_2OCH_2—[U(—CH_2OH)—CH_2OCH_2—]$_2$—U—$(CH_2OH)_2$ and $HOCH_2$—U(—CH_2OH)—CH_2—[U(—CH_2OH)—CH_2OCH_2—]$_2$—U—$(CH_2OH)_2$
551[b]	CH_2=***M***—CH_2UCH_2—***M***—CH_2UCH_2—U—CH_2OH
561	$HOCH_2$—U(—CH_2^+)—CH_2OCH_2—[U(—CH_2OH)—CH_2OCH_2—]$_2$—U—$(CH_2OH)_2$
582[b]	Same species as sample 2 (Table II) and CH_2=***M***—CH_2UCH_2—***M***(—CH_2OH)—CH_2UCH_2—U—CH_2OH and CH_2=***M***—CH_2UCH_2—***M***(—CH_2OH)—CH_2U—CH_2OCH_2—U
592	***M***—CH_2—U—CH_2—***M***—$(CH_2OH)_3$ and $HOCH_2$—***M***—CH_2—U—CH_2—***M***—$(CH_2OH)_2$
648	$(HOCH_2)_2$—U—CH_2—[—OCH_2—U(—CH_2^+)—CH_2—][—OCH_2—U—CH_2—]$_2OCH_2$—U—$(CH_2OH)_2$
697–702	$(HOCH_2)_2$—***M***—CH_2—U—CH_2—U—CH_2—U—CH_2—***M***—$(CH_2OH)_2$
782 (784[a])	CH_2=***M***—CH_2UCH_2—***M***(—CH_2OH)—CH_2UCH_2—[U(—CH_2OH)—CH_2]$_2$—U—CH_2OH and CH_2=***M***—CH_2UCH_2—***M***(—CH_2OH)—CH_2UCH_2—[U—CH_2OCH_2—]$_2$—U—CH_2OH
790[b]	Like Table II and $(HOCH_2)_3$—***M***—CH_2—U(—CH_2OH)—CH_2—[U—CH_2]$_2$—***M***—$(CH_2OH)_3$ and/or $(HOCH_2)_3$—***M***—CH_2—U—CH_2OCH_2—[U—CH_2]$_2$—***M***—$(CH_2OH)_3$ and/or $(HOCH_2)_2$—***M***—CH_2—U—CH_2OCH_2—[U—CH_2OCH_2]$_2$—***M***—$(CH_2OH)_2$
815	$(HOCH_2)_2$—***M***—CH_2—U—CH_2—U(—CH_2^+)—CH_2—U—CH_2—U(CH_2OH)—CH_2—***M***—$(CH_2OH)_2$ and $(HOCH_2)_2$—***M***—CH_2—U(—CH_2^+)—CH_2—U—CH_2—U—CH_2OCH_2U—CH_2—***M***—$(CH_2OH)_2$
905	***M***—CH_2—***M***—CH_2—U—CH_2—***M***(—CH_2OH)—CH_2—U—CH_2—[U(CH_2OH)—CH_2—]$_2$—U—CH_2OH and/or ***M***—CH_2—***M***—CH_2—U—CH_2—***M***(—CH_2OH)—CH_2—U—CH_2—[U—CH_2OCH_2—]$_2$—U—CH_2OH and/or $HOCH_2$—***M***—CH_2—***M***—CH_2—U—CH_2—***M***(—CH_2OH)—CH_2—U(CH_2OH)—CH_2—[U—CH_2—]$_2$—U—CH_2OH and/or other variations on the theme
956	Mainly CH_2=***M***—$(CH_2OH)_2$—CH_2UCH_2—***M***(=CH_2)(CH_2OH)—CH_2UCH_2—[U—CH_2OCH_2]$_3$—U—CH_2OH and/or CH_2=***M***—$(CH_2OH)_2$—CH_2UCH_2—***M***(=CH_2)(CH_2OH)—CH_2UCH_2—[U(—CH_2OH)—CH_2]$_3$—U—CH_2OH
1012	***M***—CH_2—U—CH_2—***M***—CH_2—***M***—CH_2—U—CH_2—***M***(—CH_2OH)—CH_2—U—CH_2—[U(CH_2OH)—CH_2—]$_2$—U—CH_2OH and/or another variation on the theme such as peak 905 + ***M***—CH_2—U—CH_2—
1187	Mainly CH_2=***M***—$(CH_2OH)_2$—CH_2UCH_2—***M***(=CH_2)(CH_2OH)—CH_2UCH_2—[U—CH_2OCH_2]$_5$—U—$(CH_2OH)_2$ and/or CH_2=***M***—$(CH_2OH)_2$—CH_2UCH_2—***M***(=CH_2)(CH_2OH)—CH_2UCH_2—[U(—CH_2OH)—CH_2]$_5$—U—$(CH_2OH)_2$ equivalent to 2M + 8U and/or 6M + 3U and/or $HOCH_2$—U—CH_2UCH_2—***M***(—CH_2OH)—CH_2UCH_2—***M***(—CH_2OH)—CH_2—[—***M***—CH_2—]$_3$—***M***=CH_2
1363	1187 + 1*x*(—U—CH_2—)$_2$ and + 1*x*—CH_2OH more

Urea-to-urea methylene ether structures still predominate in sample 14. ^{13}C-NMR indicates the still predominant presence of methylol groups and urea-to-urea methylene ether bridges but also the presence of a very noticeable proportion of methylene bridges. U = urea.

[a] Calculated.

[b] There may be different species of the same peak in Table I mixed with the melamine species shown in this table.

TABLE V
Relative Proportion Variations of Lower Molecular Weight Melamine Species from Sample 7 to Sample 14

Sample	***M***—$(CH_2OH)_2$	***M***—$(CH_2OH)_3$	***M***$(CH_2OH)_4$	UCH_2***M***$(CH_2OH)_3$	H(U—CH_2)$_2$***M***$(CH_2OH)_3$	H$(UCH_2)_3$***M***$(CH_2OH)_3$
7	9	23	17	54	100	12
10	24	26	32	82	100	12
14	7	8	30	20	100	9

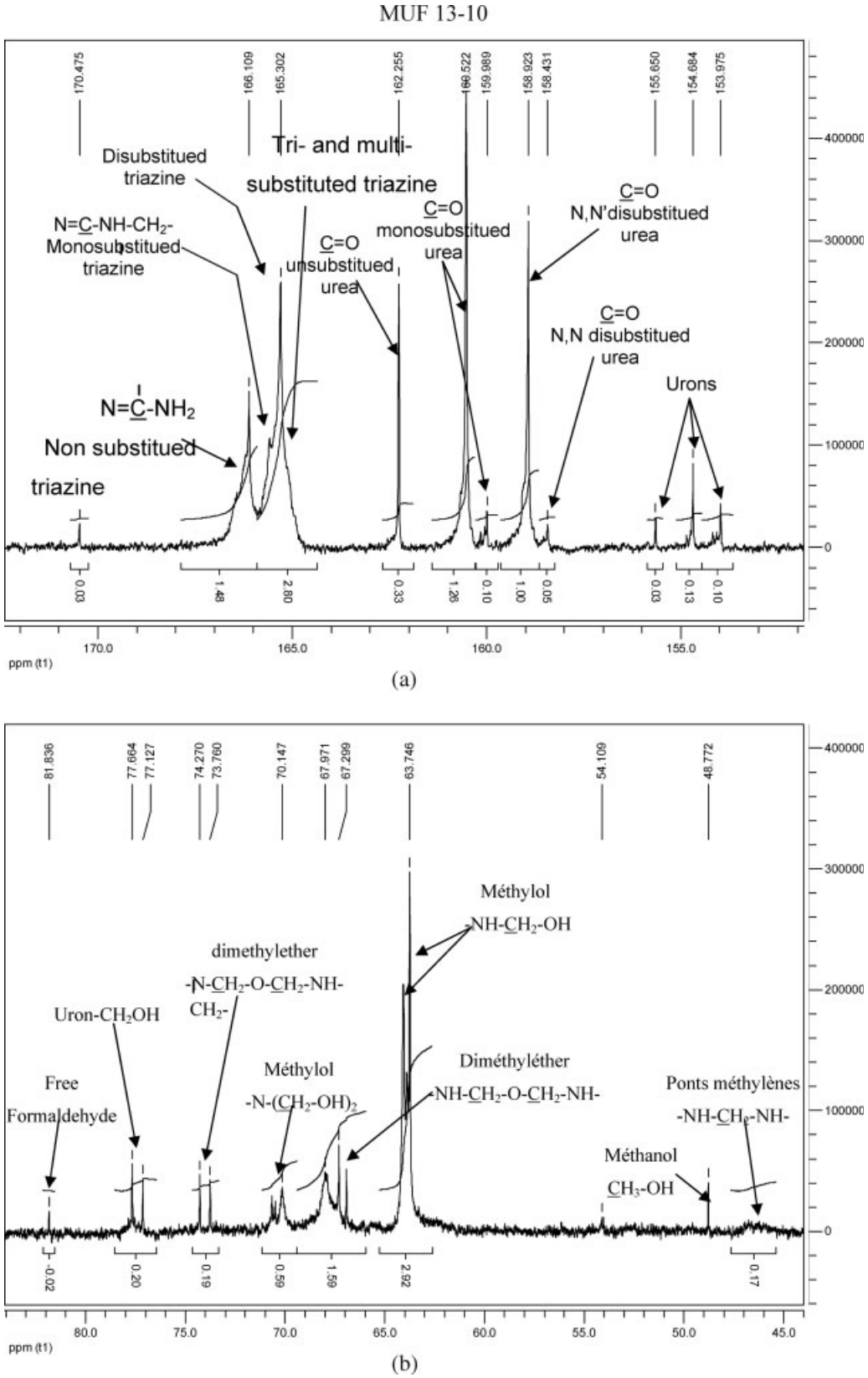

Figure 13 ^{13}C-NMR spectra of sample 10: (a) a detail of the 150–170 ppm region and (b) a detail of the 43–85 ppm region.

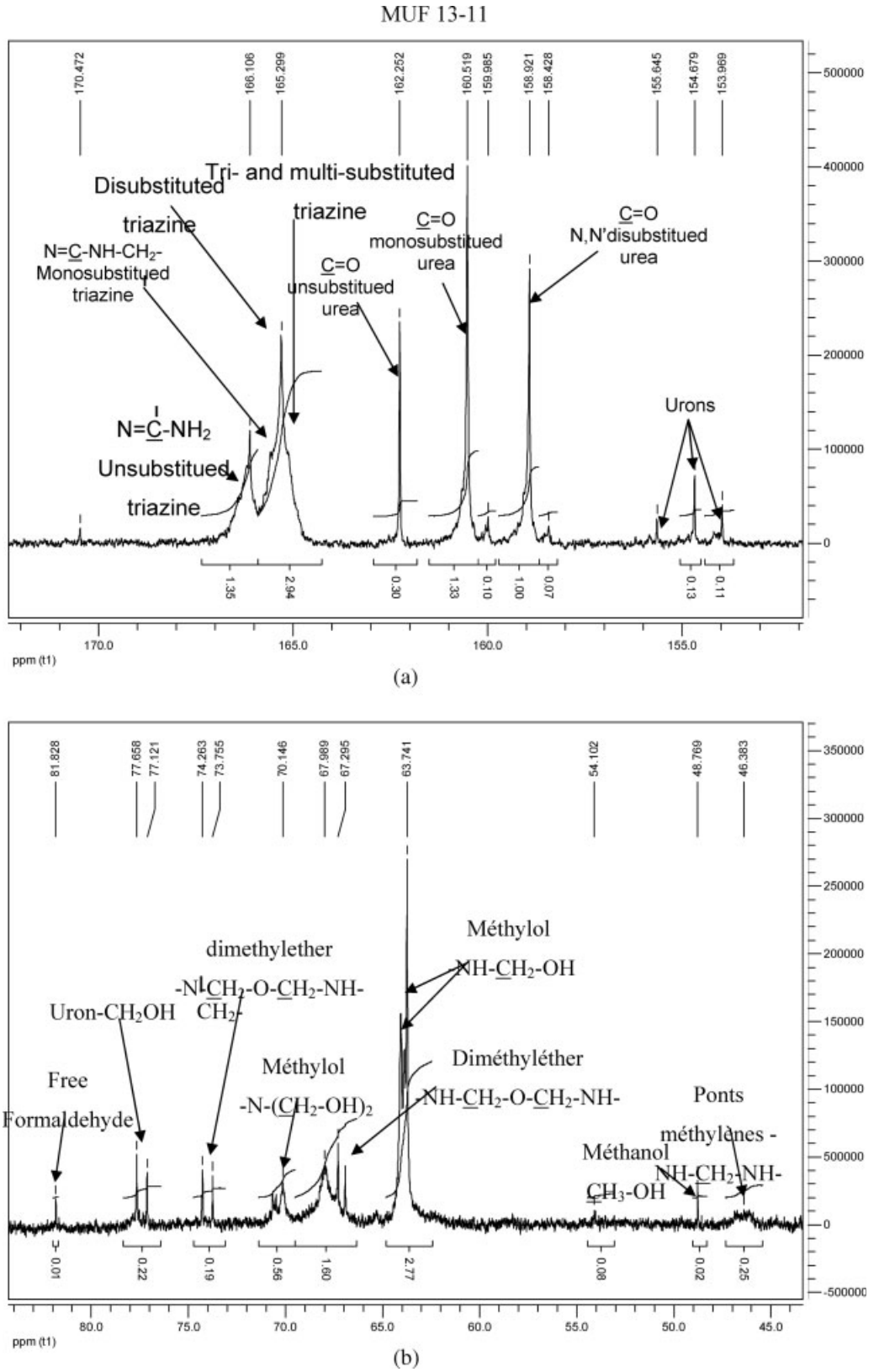

Figure 14 ^{13}C-NMR spectra of sample 11: (a) a detail of the 150–170 ppm region and (b) a detail of the 43–85 ppm region.

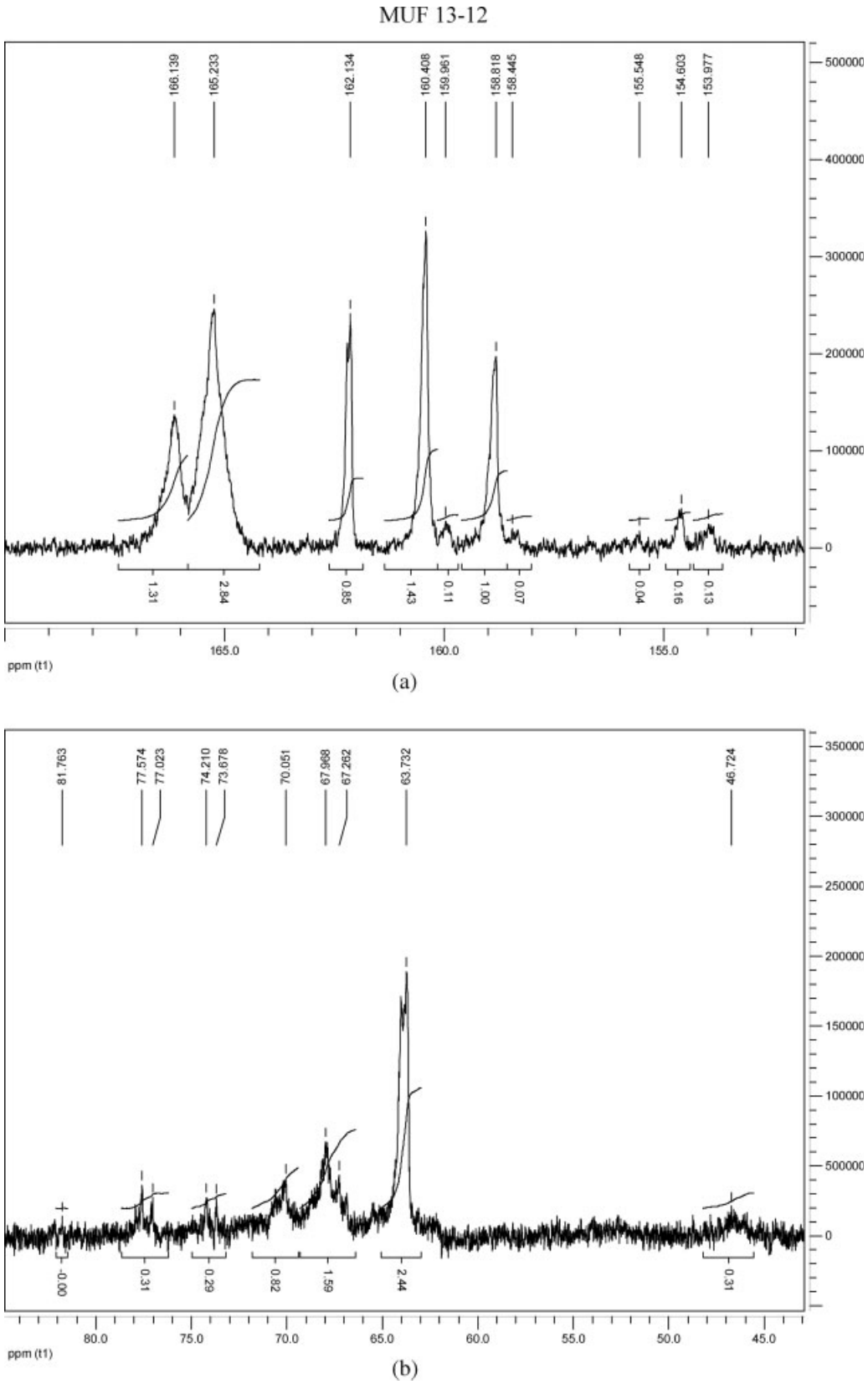

Figure 15 ^{13}C-NMR spectra of sample 12: (a) a detail of the 150–170 ppm region and (b) a detail of the 43–85 ppm region.

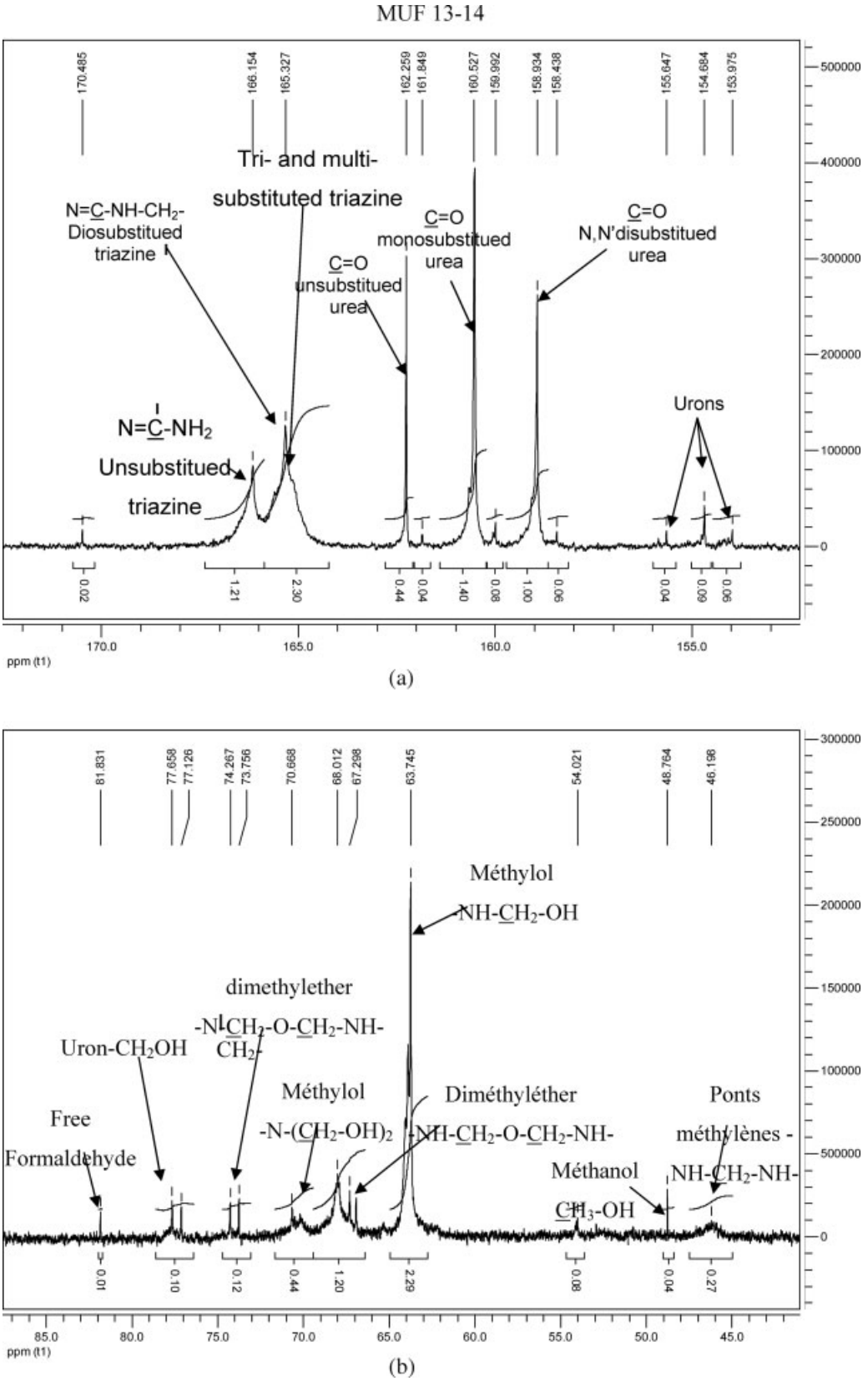

Figure 16 ^{13}C-NMR spectra of sample 14: (a) a detail of the 150–170 ppm region and (b) a detail of the 43–85 ppm region.

sample 11 to sample 12; Figs. 14(b) and 15(b)] and appears again (from sample 12 to sample 14), giving an idea of the complex equilibria involved. This shows that the introduction of melamine into the reaction induces some rearrangement of the $—CH_2OCH_2—$ bridges to $—CH_2—$ bridges with a simultaneous release of formaldehyde, which then reacts again. This alternating formation/consumption mechanism continues from sample 7 to sample 14.

Upfield, the proportions of all the species (ethers at 73–74.5 and 67 ppm and methylol urons at 77–78 ppm) other than the methylol groups, at 63–64 ppm and *N*-dimethylol groups, go up and down, passing from 10 to 11 to 12 to 14 if one compares the peak area integrals normalized for each spectrum:

$$N–CH_2OH \leftrightarrows N–(CH_2OH)_2 \leftrightarrows -CH_2–N–CH_2OH$$
$$\hookrightarrow \quad \text{to} \quad –CH_2– \quad \hookleftarrow$$

Passing from sample 10 to sample 14 [from Fig. 13(b) to Fig. 16(b)], one can notice a marked relative decrease in $—CH_2OH$ of monomethylolated urea at 64.2 ppm in relation to $—CH_2OH$ of disubstituted urea at 63.7 ppm and a relative increase in $—CH_2OH$ of melamine situated between the two peaks of the $—CH_2OH$'s of urea.

The relative proportions of monosubstituted, disubstituted, and trisubstituted melamines in the C=N parts per million range of the triazine ring is in line with what is observed by MALDI-TOF, with an apparent progressive increase in the proportion of the trisubstituted case from sample 7 to sample 14 [from Fig. 12(a) to Fig. 16(a)]. Methanol increases steadily but to a small extent from sample 1 to sample 14 because of the continuous existence of the Cannizzaro disproportionation reaction.[8–10]

In the first part of the melamine reaction (from sample 7 to sample 10), the lower molecular weight species up to 425 Da (Table VI) increase in proportion, the species at 425 to 551 Da remain approximately stable, and the higher molecular weight species decrease slightly (with the exception of the 790-Da species, which increases). Passing further from sample 10 to sample 14, we find that mixed oligomers of melamine and urea of not too high a molecular weight tend to increase in proportion, this being particularly marked for the 375- and 581-Da species. The proportion of methylolated urea species, especially of a low molecular weight, decreases markedly, especially the 143-Da species, whereas low-molecular-weight melamine and urea species decrease too as shown in Table V.

The proportions of each very high-molecular-weight species tend to either remain stable or decrease. These species proportions are already low in the beginning, but they decrease to one-third of their proportions in sample 10 by the time at which the reaction has reached the stage of sample 14. This is again an indication of continuous rearrangements and complex dynamic equilibria being present, in which the higher molecular weight methylolated species do split to form smaller compounds. Thus, from sample 10 to sample 14, the proportions of the species at 822, 1217, and 1363 Da are markedly decreased. In particular, the decrease of the 822-Da compound explains in part the increase in the proportion of the smaller 582- and 249-Da species that has been already noticed. The variations in the species proportions throughout the reaction are reported in Table VI for the sample sequence of 1, 2, 7, 10, and 14.

TABLE VI
Variation of the Species Proportions from Sample 1 to Sample 14

	Relative proportion				
Peak (Da)	1	2	7	10	14
23	9	8	10	24	13
83			10	17	7
112	12	7	26	60	47
127			14	18	24
143	70	54	19	45	26
157	25	24	29	43	40
177	100	100	100	100	100
199	100	100	100	100	100
239			17	20	5
249	58	30	27	37	42
279–281	86	64	26	35	24
311			42	62	15
353	30	30	36	65	44
375	49	44	66	70	88
381	72	78	75	75	74
407	29	40	43	61	49
425			13	14	4
455			9	9	6
551	36	24	51	51	54
582	33	42	60	47	57
767			10	10	8
782	16	14	22	20	18
790			15	25	15
822			7	8	3
956	10	7	15	12	14
1187	5	7	11	6	6
1217			6	6	0–2
1363			5	3	0–2
1430			—	7	0–2

The presence of dynamic equilibria is again indicated by (1) the expected progressive decrease of the key 143-Da $U—(—CH_2OH)_2$ species from sample 1 to sample 7 followed by (2) its increase from sample 7 to sample 10 due to the melamine-induced rearrangements of $—CH_2OCH_2—$ bridges to $—CH_2—$ bridges with the liberation of HCHO regenerating $U—(—CH_2OH)_2$ and finally (3) its decrease again

from sample 10 to 14 as it continues to react as it did in part 1. Other species present similar behavior.

References

1. Pizzi, A. Advanced Wood Adhesives Technology; Marcel Dekker: New York, 1994.
2. Mercer, A. T.; Pizzi, A. J Appl Polym Sci 1996, 61, 1687.
3. Kamoun, C.; Pizzi, A.; Zanetti, M. J Appl Polym Sci 2003, 90, 203.
4. Zanetti, M.; Pizzi, A. J Appl Polym Sci 2004, 91, 2690.
5. Zanetti, M.; Pizzi, A. Holz Roh Werkstoff 2004, 62, 445.
6. Lei, H.; Pizzi, A.; Du, G.; Despres, A. J Appl Polym Sci 2006, 100, 4842.
7. Kamoun, C.; Pizzi, A.; Zanetti, A. J Appl Polym Sci 2003, 90, 203.
8. Meyer, B. Urea–Formaldehyde Resins; Addison-Wesley: Reading, MA, 1979.
9. Pizzi, A. Wood Adhesives: Chemistry and Technology; Marcel Dekker: New York, 1983.
10. Morrison, R. T.; Boyd, R. N. Organic Chemistry; Allyn and Bacon: Boston, 1965.